

Decoherence processes in a current biased dc SQUID

J. Claudon, A. Fay, L. P. Levy and O. Buisson

CRTBT-LCM I, C.N.R.S.-Université Joseph Fourier, BP 166, 38042 Grenoble-cedex 9, France

(Dated: March 23, 2024)

A current biased dc SQUID behaves as an anharmonic quantum oscillator controlled by a bias current and an applied magnetic flux. We consider here its two level limit consisting of the two lower energy states $|0\rangle$ and $|1\rangle$. We have measured energy relaxation times and microwave absorption for different bias currents and fluxes in the low microwave power limit. Decoherence times are extracted. The low frequency flux and current noise have been measured independently by analyzing the probability of current switching from the superconducting to the finite voltage state, as a function of applied flux. The high frequency part of the current noise is derived from the electromagnetic environment of the circuit. The decoherence of this quantum circuit can be fully accounted by these current and flux noise sources.

PACS numbers: Valid PACS appear here

In the past years, coherent manipulation of two and multi-level quantum systems, efficient quantum read-outs, entanglement between quantum bits have been achieved [1, 2, 3, 4, 5, 6] demonstrating the full potential of quantum logic in solid state physics. At present, future developments require longer coherence times [8, 9, 10]. In contrast with atomic system, the huge number of degree of freedom makes its optimization a challenging problem. Up to now, the most successful strategy has been to manipulate the quantum system at particular working points where its coupling to external noise is minimal [2]. Nevertheless, experimental analysis of decoherence phenomena in superconducting circuits remains a priority for a full control of quantum experiments. Different models for the noise sources have been proposed to describe the decoherence processes acting on various qubits [7, 8, 9, 10]. However a complete and consistent understanding of decoherence remains a current and open problem. In this paper, we study decoherence processes of a phase qubit: the current biased dc SQUID.

This superconducting circuit consists of two Josephson junctions (JJ), each with a critical current I_0 and a capacitance C_0 . The junctions are embedded in a superconducting loop of inductance L_s , threaded by a flux Φ . In the limit where $L_s I_0 = \Phi_0/2$, the phase dynamics of the two junctions can be mapped onto a fictitious particle following a one dimensional path in a 2D potential [5]. If the biasing current I_b is smaller than the SQUID critical current I_c , the particle is trapped in a cubic potential well characterized by its bottom frequency $\omega_p(I_b; \Phi)$ and a barrier height $U(I_b; \Phi)$ (Fig. 1a). The quantum states in this anharmonic potential are denoted $|n\rangle$, with corresponding energies E_n , $n = 0, 1, \dots$. In the following, only the lowest states $|0\rangle$ and $|1\rangle$ will be involved. For I_b well below I_c , these two levels are stable and constitute a phase qubit.

When the bias current I_b is close to I_c , U decreases and becomes of the order of a few $\sim \hbar \omega_p$. The ground state can tunnel through the potential barrier and the SQUID switches to a voltage state [11]. The tunnelling rate γ_0 of the ground state $|0\rangle$ is given by

the well-known MQT formula for underdamped JJ [12]: $\gamma_0(I_b; \Phi) = a \omega_p \exp(-36 U / \hbar \omega_p)$, where a is of order unity.

The environment of the dc SQUID induces fluctuations of the bias current and the bias flux. In this work, we show how the current and flux noise sources can be separately quantified. This is achieved by escape measurements of the SQUID at specific working points where it is mostly sensitive to current or flux noise. Using these identified noise sources, the measured decoherence times are precisely as a function of bias current.

Experimental results are analyzed assuming a linear coupling between the SQUID and the environment degrees of freedom. We suppose that current C_I and flux C_Φ noises are generated by independent gaussian sources. Here, C_x ($x = I$ or Φ) is an operator acting on the environment. Their fluctuations are specified by the quantum spectral densities $S_x(\omega)$ [14]. In presence of flux microwave (MW) excitation, the total Hamiltonian \hat{H} in the SQUID eigenstates basis $f|0\rangle; |1\rangle$ reads: $\hat{H} = \frac{\hbar}{2} \omega_p b_z - \hbar \omega_R \cos(2\theta) b_x + \hat{H}$ where b_x and b_z are Pauli matrices and $\omega_p = (E_1 - E_0)/\hbar$. The first term is the qubit Hamiltonian and the second term describes the MW excitation of reduced amplitude ω_R at frequency ω . In this notation, ω_R is also the Rabi precession frequency for a tuned excitation ($\omega = \omega_p$). The last term is the coupling to the noise sources. For our circuit it is, within linear response,

$$\hat{H} = \frac{\hbar}{2} \omega_p b_z - \frac{\hbar}{2} \frac{r_I(\omega)}{C_0 \hbar \omega_p} C_I + \frac{\hbar}{L_s} \frac{r_\Phi(\omega)}{C_0 \hbar \omega_p} C_\Phi^i + \frac{\hbar}{2} \omega_p \frac{\partial \omega_p}{\partial I_b} C_I + \frac{\hbar}{2} \omega_p \frac{\partial \omega_p}{\partial \Phi} C_\Phi^i \quad (1)$$

where θ is the asymmetry inductance parameter (see below), $r_I(\omega) = \cos \theta + \sin \theta$, $r_\Phi(\omega) = \sin \theta$ and θ is the angle between the escape and the mean slope directions in the 2D potential [11, 15]. To first order, the transverse noise proportional to b_x only induces depolarization. The longitudinal term proportional to b_z induces "pure" dephasing. The qubit sensitivity to

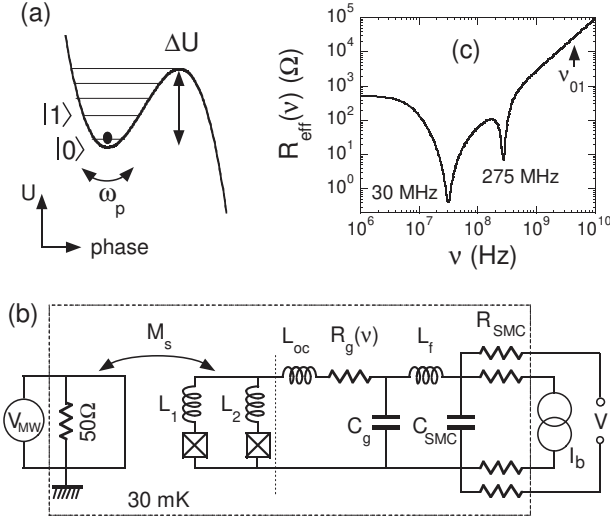


FIG. 1: (a) SQUID cubic-quadratic potential. (b) Electrical environment of the SQUID. (c) Calculated effective real impedance R_{eff} versus frequency.

longitudinal noise is given by the partial derivatives ($\partial_{\phi_1} = \partial_{I_b}$) and ($\partial_{\phi_1} = \partial_{I_b}$). They depend strongly on the experimental working point and increase near the critical current.

The measured SQUID consists of two large aluminum JJs of 15 nm^2 area ($I_0 = 1.242 \text{ A}$ and $C_0 = 0.56 \text{ pF}$) enclosing a 350 nm^2 -area superconducting loop. The two SQUID branches of inductances L_1 and L_2 contribute to the total loop inductance $L_s = 280 \text{ pH}$ with the asymmetry parameter $\epsilon = (L_1 - L_2)/L_s = 0.414$. The immediate electromagnetic environment of the SQUID is designed to decouple the circuit from the external world. It consists of two cascaded LC filters (see Fig. 1b). A large on-chip inductance $L_{\text{oc}} = 9 \text{ nH}$ is made of two long and thin superconducting wires whose value, derived from the normal state resistance, is dominated by the kinetic inductance. The gold thin film parallel capacitor, $C_g = 150 \text{ pF}$, introduces a finite resistor. Its dc value at 30 mK is $R_g = 0.1 \text{ } \Omega$ giving the gold resistivity $\rho_g = 1.2 \cdot 10^{-8} \text{ m}$. The second filter consists of the bounding wires, with an estimated inductance $L_f = 3 \text{ nH}$, and a surface mounted (SMC) capacitor $C_{\text{SMC}} = 2 \text{ nF}$ and four $500 \text{ } \Omega$ SMC resistors. The nominal room temperature microwave signal is guided by $50 \text{ } \Omega$ coaxial lines, attenuated at low temperature before reaching the SQUID through a mutual inductance $M_s = 1.3 \text{ pH}$. Special care was taken in magnetic shielding and bias lines filtering. All these electrical parameters were determined independently [11, 13]. Our environment model predicts two resonances (resistance dips in Fig. 1c). They were observed in a similar set-up and the associated resonance frequencies were in precise agreement with the model.

The current noise through the SQUID comes mostly from its immediate environment thermalized at $T =$

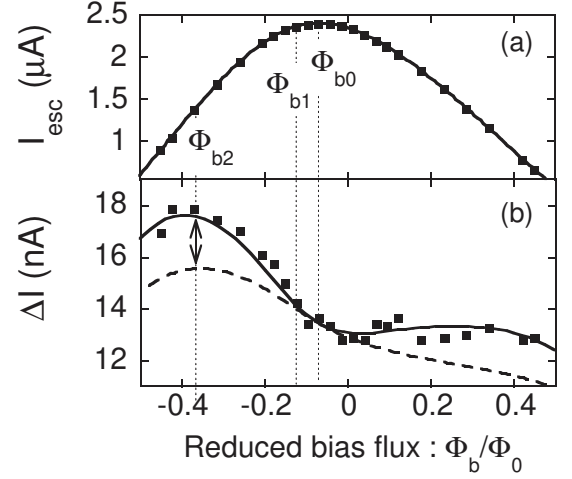


FIG. 2: (a) Measured escape current (dots) versus external applied flux fitted to MQT theory (solid line) at 30 mK . (b) The width of the probability distribution $P_{\text{esc}}(I_b)$ (dots) fitted to the 2D MQT predictions. The solid curve takes the low frequency flux noise into account while the dashed line does not. At bias flux Φ_{b0} (resp. Φ_{b1}) the sensitivity to flux noise is zero (resp. small) while it is maximum at Φ_{b2} .

30 mK ($T \ll T_c$, $T_c = 4.2 \text{ K}$, $\hbar = 6.626 \cdot 10^{-34} \text{ J s}$). The quantum spectral density of the current noise, $S_I(\omega)$ in this environment is set by the fluctuation-dissipation theorem: $S_I(\omega) = \hbar \coth \frac{\hbar \omega}{2 k_B T} + 1 R_e(\omega)^{-1}$ where $R_e(\omega)^{-1}$ is the real part of the environment circuit admittance. $R_e(\omega)$ is calculated using the electrical circuit shown in Fig. 1b and is plotted in Fig. 1c. To a good approximation, the root mean square (RMS) current fluctuations are of order $\sqrt{k_B T / L_{\text{oc}}} = 6 \text{ nA}$. Most of the noise is peaked around 30 MHz , a frequency much smaller than τ . A simple estimate of the flux noise produced by the inductive coupling to the $50 \text{ } \Omega$ coaxial line shows it can be neglected in the following.

The escape probability $P_{\text{esc}}(I_b)$ out of the superconducting states is measured at fixed flux using dc current pulses with $t = 50 \text{ ns}$ duration and I_b amplitude. Each measurement involves 5000 identical current pulses and the total acquisition time is $T_m = 10 \text{ s}$. The escape current I_{esc} is defined as the current I_b where the escape probability $P_{\text{esc}}(I_b) = 0.5$ and the width of the switching curve $I = I_h - I_l$ as the difference between the currents where $P_{\text{esc}}(I_h) = 0.9$ and $P_{\text{esc}}(I_l) = 0.1$. In Fig. 2, the dependence of I_{esc} and ΔI on Φ_b are plotted. By fitting the escape current curve $I_{\text{esc}}(\Phi_b)$, the experimental parameters of the SQUID ($I_0; C_0; L_s; \epsilon$) are determined.

Moreover, escape measurements are a sensitive tool to characterize noise (frequency range and amplitude). If noise frequencies exceed the inverse of a current pulse duration t^{-1} , the tunnel rate fluctuates during each current pulse. The escape probability is controlled by the average Φ_0 escape rate in the frequency window $[t^{-1}, \tau^{-1}]$: $P_{\text{esc}} = 1 - \exp(-\Phi_0 I_b + I; \Phi_b + t)$ [11, 16]. The current noise produced by the electrical

environment lies in this frequency interval. Its effect is to decrease $I_{\text{esc}}(b)$ by about 6 nA, the RMS current fluctuations (unobservable in Fig. 2a). Similarly, the width of the switching curve is not affected.

On the other hand, if noise frequencies are slower than t^{-1} , the tunnel rate is constant during a pulse, but fluctuates from pulse to pulse. In this limit, the escape probability becomes $P_{\text{esc}} = 1 - \exp(-I_b/I_c)$, where the statistical average is now in frequency range from T_m^{-1} to t^{-1} . To first order, low frequency noise does not affect I_{esc} , but increases the width Γ . Thus Γ is the best quantity to probe the origin and the magnitude of the low frequency fluctuations: if the flux b is set at the value b_0 which maximizes I_c , the SQUID is only sensitive to current fluctuations since $\frac{\partial I_c}{\partial b} = 0$. In the vicinity of this flux, the measured width is explained by the usual MQT theory. Hence the measured RMS current fluctuations in the $[T_m^{-1}, t^{-1}]$ interval (low frequency current noise) is below 0.5 nA, the error bar in I_c measurements. This is consistent with the 0.1 nA RMS value derived from the spectral density of noise at frequencies below t^{-1} . For other applied fluxes, the width is slightly larger than MQT prediction, indicating a residual low frequency flux noise. The dependence of Γ on b shown in Fig. 2b is perfectly explained by a gaussian low frequency flux noise. Its RMS amplitude, $\frac{2}{L_F} \Gamma^{1/2} = 5.5 \cdot 10^{-4} \phi_0$, is extracted from the Γ shown in Fig. 2b and is attributed to the flux noise in the [100 MHz; 20 kHz] frequency interval. The origin of flux noise may be due to vortices trapped in the four aluminum contact pads located at a 0.5 mm distance from the SQUID.

Hereafter we discuss dephasing and relaxation induced by the noise sources previously identified. These incoherent processes are experimentally studied with low power spectroscopy and energy relaxation measurement. As described in Ref.[5], a MW flux pulse is applied followed by a 2 ns duration dc flux pulse to perform a fast but adiabatic measurement of the quantum state of the SQUID (Fig. 3c inset). The duration $T_{\text{MW}} = 300$ ns of MW pulses is sufficient to reach the stationary state where the population p_i of the level $j|i$ only depends on ϕ and the amplitude R . The microwave amplitude R is calibrated using Rabi like oscillations[5]. In the two level experiments discussed in this paper, the measured escape probability P_{esc} induced by the dc flux pulse can be interpreted as $P_{\text{esc}} = P_{\text{esc}}^{ji} + (P_{\text{esc}}^{ji} - P_{\text{esc}}^{ji}) R(\phi; R)$. P_{esc}^{ji} denotes the escape probability out of the pure state $j|i$. In Fig. 3a and 3b, the escape probability versus microwave frequency are plotted at two different biasing points. The experimental curves present a resonant peak which position and full width at half maximum define the resonant frequency ϕ_{01} and Γ . Spectroscopy experiments are performed in the linear regime and is experimentally checked to be independent of the MW amplitude. Relaxation measurements were performed by populating the $j|i$ state with low power MW tuned at ϕ_{01}

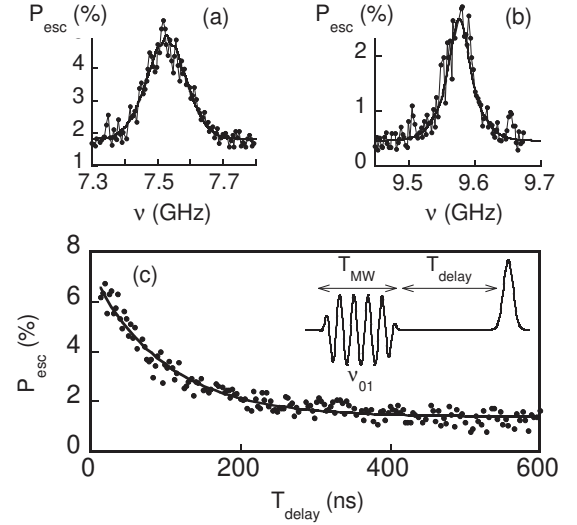


FIG. 3: (a) and (b) Escape probability versus applied microwave frequency with amplitude $R < 5$ MHz at two different working points ($I_b = 2.288$ A; $b_1 = 0.117 \phi_0$) and ($I_b = 0.946$ A; $b_2 = 0.368 \phi_0$), respectively. The points are experimental data and the continuous lines are the Fourier transforms of $f_{\text{coh}}(t)$ (see text). (c) Measured escape probability versus delay time (dots) fitted to an exponential law with $T_1 = 95$ ns (continuous line). The inset specifies the timing of the measurement pulse which follows the MW excitation pulse.

during a time $T_{\text{MW}} = 300$ ns, and measuring its population with increasing time delay T_{delay} after the end of the MW pulse. As shown in Fig. 3c, the escape probability follows an exponential relaxation with a characteristic time T_1 . In Fig. 4, measured resonant frequency ϕ_{01} , relaxation time T_1 and the inverse of microwave width Γ^{-1} are plotted versus current bias for the two different applied fluxes b_1 (close to b_0) and b_2 shown in Fig. 2. ϕ_{01} , T_1 and Γ^{-1} decreases as I_b gets closer to I_c . For these two applied fluxes, the ϕ_{01} dependence fits perfectly the semiclassical formulas for a cubic potential [17] using the same SQUID electrical parameters as those extracted from escape measurements.

The depolarization rate T_1^{-1} is given by the sum $T_1^{-1} = R + E$ of the relaxation R and the excitation E rates. These two rates are calculated using Fermi golden rule. At low temperature, excitation can be neglected and R reads:

$$R = \frac{r_I^2(\phi)}{4C_0 \hbar \omega_{01}} S_I(\phi_{01}) + \frac{r^2(\phi)}{L_s^2 C_0 \hbar \omega_{01}} S(\phi_{01}):$$

Neglecting the high frequency part of the flux noise, one obtains $T_1 = 2R_e(\phi_{01})C_0 = r_I^2(\phi)$ where $R_e(\phi_{01}) = (2L_{oc}\omega_{01})^2 = R_g(\phi_{01})$. $R_g(\phi) = R_s$ is the high frequency resistance of the gold capacitor where $R_s = \frac{\rho}{0.9}$ is the surface resistance and ρ is a dimensionless geometrical parameter. The T_1 versus I_b dependence is well fitted with $\rho = 200$ as the only adjustable parameter (Fig. 4b). This value is the right order of magnitude for the geom-

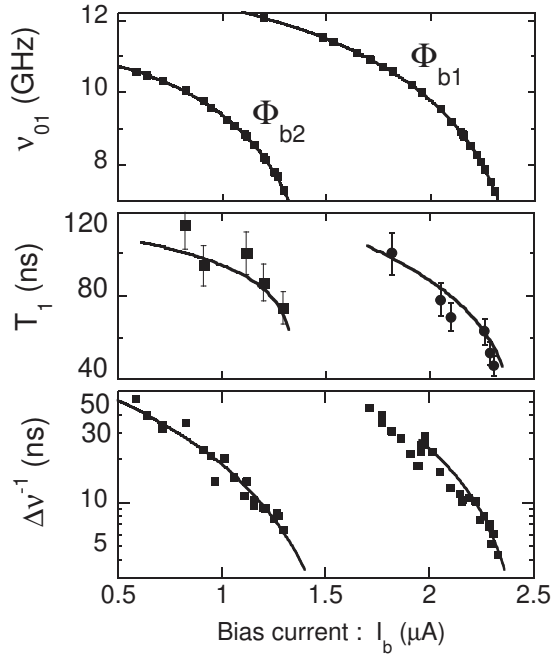


FIG. 4: Resonant transition frequency (a), relaxation time (b) and microwave width (c) as function of bias current at $b_1 = 0.117$ ϕ_0 and $b_2 = 0.368$ ϕ_0 respectively right and left curves. Symbols correspond to experiments and continuous line to model predictions.

etry of the gold capacitor.

Relaxation alone is too weak to explain the value of $\Delta\nu^{-1}$ and "pure" dephasing also contribute to the linewidths. First, we consider the time evolution of the reduced density matrix in the basis f_{ji} in the absence of MW. The linear coupling to noise sources induces a time decay of the amplitude $f_{coh}(t)$ of the coherence terms. Since current and flux noises are independent, $f_{coh}(t)$ is factorized as $f_{coh}(t) = f_I(t) f_\Phi(t) \exp(-2t/T_1)$ where $f_I(t)$ and $f_\Phi(t)$ are respectively the "pure" dephasing contributions due to current and flux noises.

The current contribution is given by the well-known gaussian noise formula [10, 18]: $f_I(t) = \exp(-\frac{1}{2}t^2/T_1^2)$

$\exp(-\frac{1}{2}t^2/T_1^2)$, where $(\phi_{01} = \phi_{Ib})$ is extracted directly from the slope of the experimental curve of Fig. 4a. We neglect flux noise contributions with frequencies higher than 20 kHz. Since the acquisition time of absorption spectra and escape measurements are similar, the SQUID undergoes the same RMS fluctuations in the two experiments. In these conditions, $f_\Phi(t)$ takes the simple gaussian form: $f_\Phi(t) = \exp(-\frac{1}{2}t^2/T_\Phi^2)$. $(\phi_{01} = \phi_{Ib})$ was computed using the known electrical parameters of the SQUID [19].

Within linear response, the shape of the resonance curve is proportional to the Fourier transform (FT) of $f_{coh}(t)$. Resonance curves in Fig. 3a and 3b are fitted using $P_{esc} = P_{esc}^{ji} / \text{FT}[f_{coh}g(\phi_{01})]$ (continuous line). Our model explains perfectly the shape of the experimental curves. In Fig. 4c, the theoretical width extracted from the curve $\text{FT}[f_{coh}g(\phi_{01})]$ is in very good agreement with experimental data without free parameter. When I_b gets close to I_c , the partial derivatives $(\phi_{01} = \phi_{Ib})$ and $(\phi_{01} = \phi_{Ib})$ increase: the noise sensitivity increases and $\Delta\nu^{-1}$ broadens. For bias points corresponding to b_2 , the width is due to current and flux noise. For a bias flux equal to b_1 , the effect of flux noise is small and the width is dominated by current noise. At this flux, for $I_b < 1.95$ A, our model predicts satellite resonances around ϕ_{01} which are not observed. Other noise mechanism may blur the predicted satellite peaks.

In conclusion, we have shown how the flux and current noise present in this controlled quantum circuit can be separately identified. We measured the decoherence times at low microwave power where the quantum circuit can be reduced to a two level system. Analyzing the coupling of the SQUID to the known noise sources, the measured relaxation times and the resonance width can be fully understood.

We thank E. Colin, V. H. Dao, K. Hasselbach, F. W. J. Hekking, B. Pannetier, P. E. Roche, J. Schrieffer, A. Shnirman for very useful discussions. This work was supported by two ACI programs and by the Institut de Physique de la Matière Condensée.

-
- [1] T. Yamamoto et al, Nature 425, 941 (2003).
 - [2] D. Vion et al, Science 296, 886 (2002).
 - [3] J.M. Martinis et al, Phys. Rev. Lett. 89, 117901 (2002).
 - [4] I. Chiorescu et al, Science 299, 1869 (2003).
 - [5] J. Claudon et al, Phys. Rev. Lett. 93, 187003 (2004).
 - [6] A. Wallraef et al, Nature 431, 162 (2004).
 - [7] K.B. Cooper et al, Phys. Rev. Lett. 93, 180401 (2004).
 - [8] O. Astaev et al, Phys. Rev. Lett. 93, 267007 (2004).
 - [9] P. Bertet et al, cond-mat/0412485.
 - [10] G. Ithier et al, Phys. Rev. B 72, 134519 (2005).
 - [11] F. Balestro et al, Phys. Rev. Lett. 91, 158301 (2003).
 - [12] A.O. Caldeira and A.J. Leggett, Ann. Phys. 149, 374 (1983).
 - [13] J. Claudon, PhD Thesis, Université Joseph Fourier, Grenoble, France (2005).
 - [14] The quantum spectral density is defined as follows: $S_x(\omega) = \int_{-\infty}^{\infty} dt \langle C_x(0) C_x(t) \rangle e^{i\omega t}$.
 - [15] V. Lefevre-Seguin et al, Phys. Rev. B 46, 5507 (1992).
 - [16] J.M. Martinis and H. Grabert, Phys. Rev. B 38, 2371 (1988).
 - [17] A.I. Larkin and Y.N. Ovchinnikov, Sov. Phys. JETP 64, 185 (1986).
 - [18] A. Cottet, PhD thesis, Université Paris VI, (2002).
 - [19] $(\phi_{01} = \phi_{Ib})$ could be measured by changing slightly I_b . In fact, we kept I_b as constant as possible during experiments, because of a static flux hysteresis about 10^{-3} ϕ_0 .